



# POD surrogate models using adaptive sampling space parameters for springback optimization in sheet metal forming

Van Dang, Carl Labergere, Pascal Lafon

## ► To cite this version:

Van Dang, Carl Labergere, Pascal Lafon. POD surrogate models using adaptive sampling space parameters for springback optimization in sheet metal forming. *Procedia Engineering*, 2017, 207, pp.1588 - 1593. 10.1016/j.proeng.2017.10.1053 . hal-03609562

**HAL Id: hal-03609562**

**<https://hal.science/hal-03609562>**

Submitted on 15 Mar 2022

**HAL** is a multi-disciplinary open access archive for the deposit and dissemination of scientific research documents, whether they are published or not. The documents may come from teaching and research institutions in France or abroad, or from public or private research centers.

L'archive ouverte pluridisciplinaire **HAL**, est destinée au dépôt et à la diffusion de documents scientifiques de niveau recherche, publiés ou non, émanant des établissements d'enseignement et de recherche français ou étrangers, des laboratoires publics ou privés.

International Conference on the Technology of Plasticity, ICTP 2017, 17-22 September  
2017, Cambridge, United Kingdom

## POD surrogate models using adaptive sampling space parameters for springback optimization in sheet metal forming

Van Tuan Dang\*, Carl Labergere, Pascal Lafon

*University of Technology of Troyes, Charles Delaunay Institute (ICD)/Laboratory of Mechanical Systems and Concurrent Engineering  
(LASMIS), UMR CNRS 6281, 12 Rue Marie Curie, CS 42060, 10004 Troyes Cedex, France*

---

### Abstract

The use of high strength steels for the stamping process in automotive body parts requires master spring back effects. Several parameters of the stamping process have an influence on springback effects. It is possible to optimize these parameters, but only way to achieve this optimization procedure is to use numerical simulation of the stamping process. Nevertheless, the optimization process requires an expensive evaluation of a high fidelity model over the whole design space. To reduce the overall computational cost, a surrogate model for the optimization process replaces the high fidelity model. Extensive design of numerical experiments on the overall design space of the high fidelity model is needed to build this surrogate model. To improve the efficiency of the overall optimization process, this paper presents Proper Orthogonal Decomposition (POD) surrogate models using adaptive sampling design space. Here the POD surrogate model aims to represent the final displacement field from the initial high-fidelity simulation and use the reduced basis and the radial basis functions (RBF) interpolation of the POD coefficient to describe and predict the final shape. During the optimization process, the new samples of the high-fidelity model are added using the minimization of the predicted objective function criterion. The proposed methodology is illustrated with the “U-bend” from the Numisheet2011 benchmark. Two parameters, the blank holder force and die radius are chosen to optimize the spring back effect.

© 2017 The Authors. Published by Elsevier Ltd.

Peer-review under responsibility of the scientific committee of the International Conference on the Technology of Plasticity.

**Keywords:** Proper orthogonal decomposition, Radial basis function, Surrogate model, Stamping process, Springback, Design optimization.

---

---

\* Corresponding author. Tel.: +33-325-717-600; fax: +33-325-717-600.

E-mail address: [van\\_tuan.dang@utt.fr](mailto:van_tuan.dang@utt.fr)

## 1. Introduction

In mechanical systems, the rational use of experimental tests to optimize manufacturing processes is very old. Nowadays, highly efficient numerical simulations thanks to their high progress can replace the experiments. However, due to significant long computational time, especially for more predictive models, it is difficult to perform a high-fidelity numerical simulation in optimization process of metal forming which requires simulation for each iteration. Surrogate model is necessary to provide an approximation of a selected objective function over the whole design space and find an optimal design candidate. However, instead of using the scalar quantities in an optimization process the objective [1], this approach proposes a common practice in building surrogate model based on the Proper Orthogonal Decomposition (POD) method [2] for the final displacement field. This displacement field is decomposed in a combination of restricted modes, which are calculated from the covariance matrix built through snapshots of the Finite Element (FE) fields of the high-fidelity model (HFM) simulation. In this work, POD basis is computed based on the snapshot method [3] and Radial Basis Function (RBF) networks [4] is built for POD coefficient interpolation over the parameter space. Then, the full displacement field is reconstructed by using a several basis vector which is able to describe the final shape after springback.



Fig. 1: Sampling for optimization in parameter space  $D$ . (a) Apriori sampling  $D_s$ . (b) Adaptive sampling, ● initial parameters, ■ optimal parameters, — optimization trajectory, ○ sample parameters.

The aim of this paper is the development of optimization method to control the springback effect after stamping operation of automotive body part. This method is based on POD surrogate model to replace the FEM-HFM and to reduce the computational cost. Firstly, a surrogate model will be built from evaluating the set of initial Design of Experiment (DoE) samples through the HFM simulation. Then, an offline-online approach will be proposed for an optimization framework over the design space. An adaptive HFM sample from an *a priori* sampling (see Fig. 1a) will be added by a greedy algorithm [5] based on the predicted objective function criterion. This procedure will be stopped after some iterations as soon as the objective function obtains a desirable value. Finally, an optimization trajectory in the parameter space is illustrated in Fig 1b showing an optimal design of the sheet metal forming process.

## 2. Surrogate model based on POD-RBF

### 2.1. Proper orthogonal decomposition for the parametric problem

We define firstly the function over the parameter space:

$$\begin{aligned} u : D &\rightarrow R^d \\ \theta &\rightarrow u(\theta) \end{aligned}$$

which is a HFM simulation defined in the parametric space  $D$ . Each displacement vector  $u(\theta)$  is a discrete representation of the Finite Element (FE) fields and  $d$  is the number of the degrees of freedom or number of nodes. The  $d$ -dimensional vector state solution called snapshots and is denoted by  $u_i = u(\theta_i)$ . Set of snapshot vectors in  $R^d$  is obtained from the HFM simulation by  $S^N = \{u_1, u_2, \dots, u_N \in R^d\}$ , where  $N$  is number of snapshots ( $N \leq d$ ). The POD allows finding a reduced order model (ROM) by projecting the HFM computed solution onto a set of optimal orthogonal basis vectors (called POD modes), which consist of a lower-dimensional subspace. To build the ROM, the  $d \times N$  deviation matrix  $D_u = \{u_1 - \bar{u}, u_2 - \bar{u}, \dots, u_N - \bar{u}\}$  is firstly computed where  $\bar{u}$  is the snapshot mean. Next, we compute the correlation matrix  $M_u = D_u^T \cdot D_u$ , which allows finding the eigenvectors  $v^k$  and the eigenvalues  $\lambda^k, k = 1, 2, \dots, N$ . The POD basis vector  $\Psi^k$  is obtained from these eigenvectors (showed in [6]) and then each POD coefficient  $\alpha_k$  is computed by projecting the snapshots on the POD basis vector. They are defined as follows:

$$\Psi^k = \frac{1}{\sqrt{\lambda^k}} \sum_{i=1}^N (v^k)_i (u_i - \bar{u}) \text{ and } \alpha_k(\theta_i) = (u_i - \bar{u})^T \cdot \Psi^k, \quad k=1,2,\dots,N \quad (1)$$

The eigenvalues  $\lambda^k$  can be indexed in decreasing order  $\lambda^1, \lambda^2, \dots, \lambda^N$ . The rank of truncation  $K$  (called number of POD modes) can also be calculated in order to investigate whether the projection of all the pairs  $(u_i - \bar{u})$  on the linear span of the eigenvectors leads to projection errors. Thus, the error criterion  $\varepsilon(K)$  and the POD reconstruction  $u_i^{pod}$  of displacement vector of  $K$  modes are defined as follows:

$$\varepsilon(K) = 1 - \frac{\sum_{k=1}^K \lambda^k}{\sum_{k=1}^N \lambda^k} \leq \varepsilon \text{ and } u_i^{pod} = \bar{u} + \sum_{k=1}^K \alpha_k(\theta_i) \cdot \Psi^k, \quad i=1,2,\dots,N \quad (2)$$

where  $\varepsilon \in [0,1]$  is the energy threshold. Then, the RBF network will be used to interpolate the POD coefficients over the full parameter space combined with POD basis to build the surrogate model.

## 2.2. POD coefficient interpolation using RBF network.

The RBF network can be seen as a simple artificial neural network consisting of a single hidden layer of nonlinear processing units, an input layer of source nodes which is a set of  $N$  points  $\theta_i$  in a multidimensional space and an output linear weights line vector of response  $y$  represented as a linear combination of  $N$  radial basis function:

$$y(\theta) = \sum_{i=1}^N w_i h(\|\theta - \theta_i\|) \quad (3)$$

where  $h$  is the radial basis function and  $\|\cdot\|$  denotes the Euclidean norm. Each RBF is associated to a different center and is weighted by a coefficient  $w_i$ . This function measures the distance  $\|\theta - \theta_i\|$  between a current set of parameters and the reference parameter vector  $\theta_i$ . The weight coefficients  $w_i$  are determined by ensuring that the values of the interpolation function match exactly the given data  $A$ . This is achieved by enforcing  $y(\theta) = A$  which produces a linear equation  $A = B \cdot W$ , where  $A = [a_1, a_2, \dots, a_N]^T$  and  $B = (b_{ki}) \in R^{N \times N}$  is the matrix of the interpolation functions which contains the vector  $b_{ki} = h(\|\theta_k - \theta_i\|)$ ,  $i, k = 1, 2, \dots, N$ . Finally,  $W = [w_1, w_2, \dots, w_N]^T$  are then determined by solving the linear system  $W = B^{-1} \cdot A$ . The accuracy of the RBF interpolation depends highly on the choice of the radial functions. There are some forms which can be chosen, for example, Gaussian functions, Multiquadric, Inverse quadratic, Inverse Multiquadric, etc. In this work, the Multiquadric function is chosen as the radial function for training the RBF model. The input is the parameter space and the output are the POD coefficients. Finally, the surrogate model based on POD-RBF of order  $K$  at any point in the parametric space  $\theta$  is expressed as:

$$\hat{u}(\theta) = \bar{u} + \sum_{k=1}^K \hat{\alpha}_k(\theta) \cdot \Psi^k \quad (4)$$

where the expansion coefficients  $\hat{\alpha}_k(\theta_i)$  are interpolated by the RBF model over full parametric space.

## 3. The optimization framework

### 3.1. Formulation problem.

The springback optimization problem can be defined as follow:

$$\min_{\theta \in D} F(u(\theta), \theta) \quad (5)$$

where  $F(.,.)$  is the objective function,  $\theta \in D$  is a vector of optimized variables,  $u \in R^d$  is a vector of the displacement field coming from the output of the HFM simulation. In this case, the objective function can be seen as a mean of the magnitude of the displacement field between the final shape and the target shape. The magnitude  $U_i$  of the arbitrary nodal displacement is defined by:

$$U_i(\theta) = \sqrt{(x_i(\theta) - x_i^0)^2 + (y_i(\theta) - y_i^0)^2 + (z_i(\theta) - z_i^0)^2}, i = 1, 2, \dots, N_{nodes} \quad (6)$$

where  $(x_i, y_i, z_i)$  and  $(x_i^0, y_i^0, z_i^0)$  are the coordinates of the final shape and the target state at  $i$ -th node,  $N_{nodes}$  is the number of nodes of the displacement field. Then, the objective function (6) is expressed as follows:

$$F(u(\theta), \theta) = \frac{1}{N_{nodes}} \sum_{i=1}^{N_{nodes}} U_i(\theta) = \frac{1}{N_{nodes}} \sum_{i=1}^{N_{nodes}} \sqrt{(x_i(\theta) - x_i^0)^2 + (y_i(\theta) - y_i^0)^2 + (z_i(\theta) - z_i^0)^2} \quad (7)$$

and typical surrogate model-based optimization problem therefore becomes:

$$\min_{\theta \in D} F(\hat{u}(\theta), \theta) \quad (8)$$

### 3.2. Online-offline procedure for adaptive approach.

This procedure requires first a number of HFM samples to build the POD surrogate model  $\hat{u}(\theta)$ . Then, the  $F(\hat{u}(\theta), \theta)$  will be computed over the design space  $D_s \subset D$  (see Fig. 1a) based on this surrogate model. The new sample is chosen automatically for the HFM simulation from the *a priori sampling* by a *greedy algorithm* based on an indicator from the minimization (8). With each new HFM sample is evaluated, the POD method adds a new snapshot allowing to obtain a new POD basis and new POD coefficients (1). The convergence of the approach is only reached when the objective function value (7) is smaller than a magnitude threshold. The whole procedure is detailed in Algorithm 1 which is implemented in Matlab with an interface to Abaqus to solve the optimization problem.

---

#### Algorithm 1: POD greedy algorithm for online-offline approach

---

**Input:** Parameter domain  $\theta \in D$ , threshold  $\eta$ , maximum iteration  $I_{\max}$

**Output:** Objective function  $F(u(\theta), \theta)$

1. Choose the initial parameters sample  $\theta \in D$  and compute the HFM  $u(\theta)$  associated with samples  $\theta$
  2. Construct the reduced basis  $\Psi$  and expansion coefficient  $\hat{\alpha}_k$  by POD using HFM  $u(\theta)$  (eq. 1)
  3. Construct the surrogate model from  $\Psi$  and  $\hat{\alpha}_k$  (eq. 4)
  4. Randomly select a set of  $N_s$  *a priori sampling*  $D_s = \{\theta_j, j=1, 2, \dots, N_s\} \subset D$
  5. **for**  $i_{\text{iter}} = 1$  to  $I_{\max}$  **do**
  6.     **for**  $j=1$  to  $N_s$  **do**
  7.         Compute the surrogate model solution  $\hat{u}(\theta_j)$  for the parameter  $\theta_j$  at  $i_{\text{iter}}$
  8.         Compute indicator from the predicted objective function minimization:  $F(\hat{u}(\theta_j), \theta_j), \theta_j \in D_s$
  9.     **end for**
  10. Find  $\theta_{i_{\text{iter}}} = \arg \min F(\hat{u}(\theta), \theta), \theta \in D_s$  (eq. 8)
  11. Compute HFM  $u(\theta_{i_{\text{iter}}})$  associated with the sample  $\theta_{i_{\text{iter}}}$
  12. Compute the objective function  $F(u(\theta), \theta)$  (eq. 7)
  13. **if**  $F(u(\theta), \theta) \leq \eta$  **then**
  14.     **break**
  15. **end if**
  16. Construct  $\Psi$  and  $\hat{\alpha}_k$  at  $i_{\text{iter}}$  by POD adds a new snapshot  $u(\theta_{i_{\text{iter}}})$  then set  $\Psi = \Psi_{i_{\text{iter}}}, \hat{\alpha}_k = \hat{\alpha}_{k(i_{\text{iter}})}$
  17.  $D_s = D_s - \{\theta_{i_{\text{iter}}}\}$
  18. **end for**
-

#### 4. Application: U shaped draw bending

The case studied in this paper is a benchmark problem of NUMISHEET 2011 [7] and it is the springback behavior of advanced high strength steels like DP780 steel in U-shaped draw bending. The DP780 steel sheet with 1.4 mm thickness, 360 mm length, and 30 mm width is used.

##### 4.1. Numerical model of the draw bending process.

The main tooling set-up and modelling of the draw bending process is shown in Fig. 2a. In this study, the modelling and the numerical simulation are performed using the FEM implemented in ABAQUS-CAE<sup>TM</sup> 6.13-1. The blank is modelled with 1935 S4R-shell elements with 7 integration points through thickness. The plastic criteria  $f$  is based on Hill'48 stress norm  $\sigma^{Hill}$  and the isotropic hardening  $R$  is described by a Swift function:

$$f(\sigma, p) = \sigma^{Hill} - R(p) \leq 0 \text{ with } R(p) = 1278.793(p + 0.0027)^{0.142} \quad (9)$$

where  $p$  is the cumulated plastic strain. Details on material's constant are provided in the benchmark material data sheet [7]. The nominal material properties of the blank are given in Table 1. All tools are assumed to be rigid bodies. The applied boundary conditions are demonstrated in Fig. 2a. Contact interaction is modelled by using the penalty contact enforcement method, which is a type of surface-to-surface contact and it is applied between the blank surface and the tool's surfaces.

Table 1. Mechanical properties of DP780.

Young's modulus(GPa)	Poisson's ratio	Yield strength(MPa)	Tensile strength(MPa)	Uniform elongation (%)	R-value
198.8	0.3	550	840	13.1	0.781

The process is executed into two different steps. The first step is to simulate the forming operation via dynamic explicit solver. The punch moves vertically until 78.1mm of displacement. The simulation of the springback is performed in the second step through a static implicit procedure. The final shape of the part is obtained after releasing the tools.

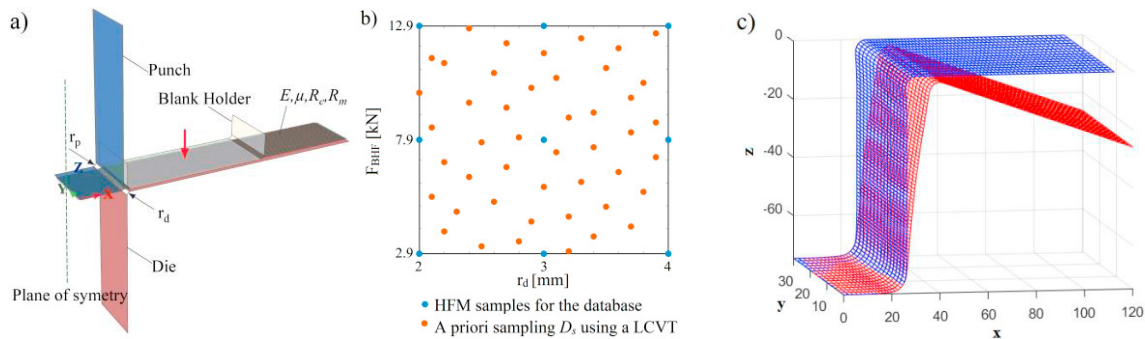


Fig. 2: (a) Numerical model of the draw bending process; (b) Design space; (c) Example of U-shape after springback.

The problem is parameterized by 2 parameters, the blank holder force  $F_{BHF}$  and the die radius  $r_d$ . In Fig. 2b, these two parameters are defined in  $D = [2, 4] \times [2.9, 12.9] \text{ (mm} \times \text{kN)}$ . A full factorial design with 9 initial points is used to build the database for the surrogate model. The sample locations are determined by a priori sampling  $D_s$  using a “Latin Centroidal Voronoi Tessellations” (LCVT) [8] with 46 points in Fig. 2b. The other parameters given include the friction coefficient  $\mu=0.1$  between the tools and blank, the thickness blank  $t=1.4$  mm and the punch radius  $r_p = 5$  mm.

## 4.2. Optimization results

The analyzed displacement field is a bi-dimensional vector field with bi-dimensional vector field, x-direction and z-direction. (In the reference frame of Fig. 2c, the displacement field in the y-direction is very weak). The POD surrogate model is built from two component of the displacement field. Thus, the objective function is compacted in bi-dimension x- and z-. The springback profile is only considered at the center nodes, which is extracted from nodes number of the numerical model of the draw bending process. The magnitude threshold was set to  $\eta=0.5$  mm for the convergence of the algorithm. The springback profiles after the U-draw bending is illustrated in Fig. 3a. We notice that the springback profile is approximated to the target profile after 6 iterations. The evaluation of the “true” objective function (7) and the “predicted” objective function (8) is plotted in Fig. 3b. The value of the “predicted” objective function is lower and close to the value of the “true” objective function and the value of the objective function is 0.41 mm using 6 HFM queries. When the convergence of the algorithm is achieved, the optimal parameters are  $\theta=(r_d, F_{BHK})=(2.1 \text{ mm}, 5.4 \text{ kN})$ . This result shows that the proposed method provides a very efficient optimization to reduce the computational cost.

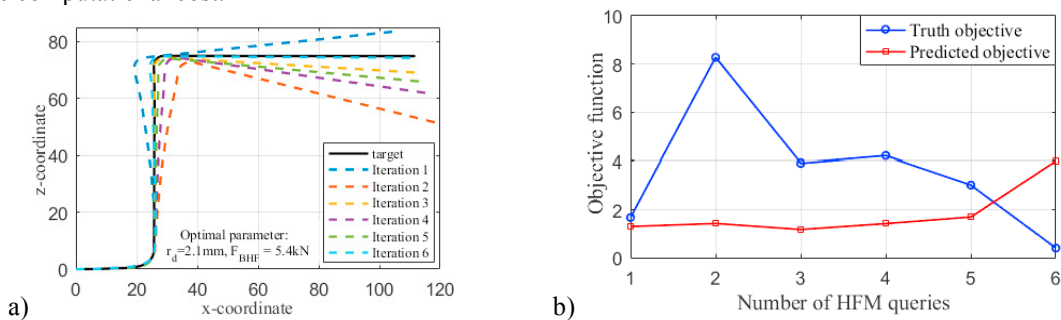


Fig. 3: (a) Springback optimization progression; (b) Convergence of objective function.

## 5. Conclusion

In this paper, we have proposed an optimization framework using an adaptive sampling from a set of candidate parameters for the springback of the metal forming process. This approach is based on the POD method combined with the RBF network to build the surrogate model. The candidate parameters are determined a priori by sampling the design parameter using technique LCVT. The results show that the proposed method is very efficient for the optimization of the U-draw bending numerical simulation of DP780. The resulting optimization is able to provide the optimal design while reducing the number of high-fidelity model simulation queries over the design space using techniques such as uniform sampling, Latin hypercube sampling or Monte Carlo sampling, etc.

Future work include the development of multilevel optimization algorithms for the metal forming processes and extension to the multi-parametric case (e.g. forming condition, tool or blank geometry and also material properties).

## References

- [1] P. Lafon, P.-A. Adragna, and V.-D. Nguyen, Multi-objective optimization under uncertainty for sheet metal forming, MATEC Web of Conferences, 80, p. 10004 (2016).
- [2] A. Chatterjee, An introduction to the proper orthogonal decomposition, Current science, 78, 808–817 (2000).
- [3] L. Sirovich, Turbulence and the Dynamics of Coherent Structures, Part1: Coherent Structures, Quarterly of Applied Mathematics 3. Brown University, Division of Applied Mathematics, 45, 561–571 (1987).
- [4] M. D. Buhmann, Radial basis functions: theory and implementations, Cambridge Monographs on Applied and Computational Mathematics, 37, 8930–8945 (2013).
- [5] S.A. Curtis, The classification of greedy algorithms, Science of Computer Programming 49, 125 – 157 (2003)
- [6] F. Vuyst and C. Audouze, Optimisation multidisciplinaire en mécanique 2, chapitre 2, LAVOISIER, 73–122(2009).
- [7] S. Huh and C. K, Benchmark study of the 8th international conference and workshop on numerical simulation of 3D sheet metal forming processes, Proceedings of Numisheet 2011, 37, 8930–8945 (2011).
- [8] Saka Y, Gunzburger M, Burkardt J (2007) Latinized, improved lhs, and cvt point sets in hypercubes. Int J Numer Anal Model 4(3–4):729–743.